

## Magnesian staurolite in garnet-corundum rocks and eclogite from the Donghai district, Jiangsu province, east China

MASAKI ENAMI

Department of Earth Sciences, School of Science, Nagoya University, Nagoya 464, Japan

QIJIA ZANG

Department of Geology, Beijing University, Beijing, China

### ABSTRACT

Magnesian staurolite of  $X_{\text{Mg}} = 0.68\text{--}0.74$  was found in garnet-corundum rocks and eclogite from the Donghai district, Jiangsu province, east China. The garnet-corundum rocks consist mainly of primary garnet, corundum, zoisite, and Na-rich phlogopite ( $\text{Na}_2\text{O} = 2.7 \pm 0.2$  wt%), with secondary magnesian staurolite, chlorite, Al-rich pargasite ( $\text{Al}_2\text{O}_3 = 22.4$  wt% maximum) and Mg-rich allanite ( $\text{MgO} = 6.2$  wt% maximum). The eclogite is composed mainly of primary garnet, clinopyroxene, corundum, kyanite, and Cr-rich zoisite ( $\text{Cr}_2\text{O}_3 = 1.6$  wt% maximum) with secondary magnesian staurolite and calcic amphibole. Equilibrium conditions of primary minerals were estimated at about  $800\text{--}850^\circ\text{C}$  and  $11\text{--}30$  kbar for the garnet-corundum rocks and  $700\text{--}750^\circ\text{C}$  and  $11\text{--}25$  kbar for the eclogite. The magnesian staurolite occurs as pseudomorphs after garnet, corundum, and kyanite. Equilibrium pressure of the magnesian staurolite is more than 11 kbar. Its equilibrium temperature is slightly lower than that of the primary minerals.

Cell dimensions of the magnesian staurolite of  $X_{\text{Mg}} = 0.74$  are  $a = 7.873(3)$  Å,  $b = 16.557(7)$  Å, and  $c = 5.637(3)$  Å. Its  $b$  axis is distinctly shorter than that of Mg-poor staurolite.  $\text{Cr}_2\text{O}_3$  content of the magnesian staurolite reaches 1.2 wt%. The Mg enrichment of staurolite is controlled by the Mg substitution for  $^{\text{VI}}\text{Al}$  and by the  $\text{Mg} = \text{Fe}$  substitution in the  $^{\text{IV}}\text{Fe}$  sites.

### INTRODUCTION

Staurolite is a common constituent mineral of pelitic and other aluminous rocks metamorphosed under intermediate pressure and temperature conditions. Staurolite is characteristically lower in  $X_{\text{Mg}}$  [=  $\text{Mg}/(\text{Mg} + \text{Fe})$ ] value than the coexisting silicate minerals: its  $X_{\text{Mg}}$  value is usually less than 0.3 (e.g., Deer et al., 1982). Iron-free staurolite (i.e., the pure-Mg end member) was synthesized under the conditions of  $T = 700\text{--}950^\circ\text{C}$  and  $P > 11$  kbar by Schreyer (1967) and Schreyer and Seifert (1969). Hellman and Green (1979) experimentally produced Mg-rich staurolite ( $X_{\text{Mg}} = 0.53\text{--}0.57$ ) from olivine tholeiitic materials under the conditions of  $T = 740\text{--}760^\circ\text{C}$  and  $P = 24\text{--}26$  kbar. These experimental works suggest that Mg-rich staurolite could occur in Mg- and Al-rich metamorphic rocks that formed at high temperature and pressure. Recently, Mg-rich staurolites have been found from various types of rock metamorphosed under high pressures ( $X_{\text{Mg}} = 0.43\text{--}0.56$ , Ward, 1984a; 0.49, Schreyer et al., 1984; 0.40–0.42, Grew and Sandiford, 1984; 0.52, Nicollet, 1986). These Mg-rich staurolites always coexist with corundum. A silica-undersaturated environment is also required for the formation of Mg-rich staurolites (e.g., Schreyer, 1967).

In the course of our petrologic study on eclogite and

the associated rocks in the Donghai district, Jiangsu province, east China, magnesian staurolite ( $X_{\text{Mg}} = 0.68\text{--}0.74$ ) was found in garnet-corundum rocks and eclogite. This is the most Mg-rich natural staurolite, as far as we know, among staurolites reported. The mode of occurrence, chemistry, crystallographic data and petrogenesis of the magnesian staurolite are described in the present paper.

### GEOLOGIC SETTING AND PETROGRAPHY

Magnesian staurolite was found in two garnet-corundum rocks and an eclogite, from the Zhimafang and Mengzhong areas in the Donghai district, respectively. Figure 1 shows a geologic sketch map of east China. The Precambrian basement of east China is divided into two units by the Tancheng-Lujiang fracture zone, i.e., an eastern unit (the Jiaoliao massif, age  $1300\text{--}2400$  Ma), and a western unit (the Jilu massif, age  $>2400$  Ma) (Tectonic map compiling group, Institute of Geology, Academia Sinica, 1974). The Donghai district is situated about 50 km east of the Tancheng-Lujiang fracture zone and belongs to the Jiaoliao massif. This district is underlain by pelitic and mafic gneisses and serpentized ultramafic rocks.

The garnet-corundum rocks and eclogite occur as sub-rounded blocks (diameter, 5–50 cm) in ultramafic rocks

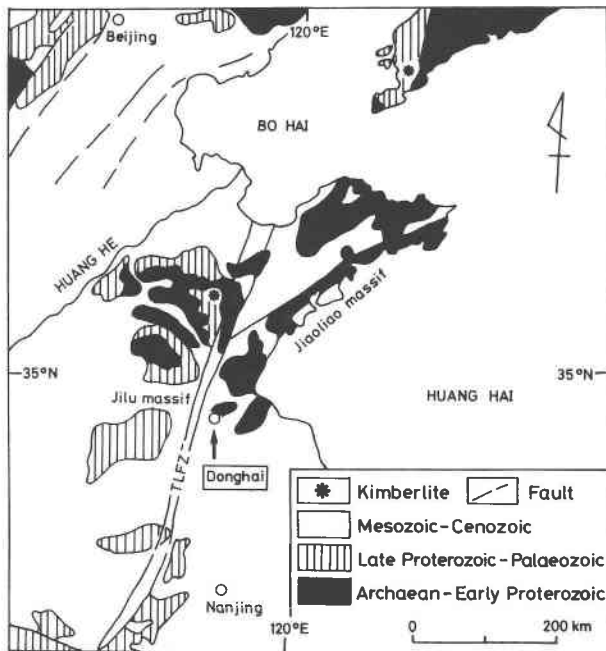


Fig. 1. Geologic sketch map of east China (simplified from Research Institute of Geology, Chinese Academy of Geological Sciences, 1982). TLFZ: Tancheng-Lujiang fracture zone.

intruding the Precambrian pelitic gneisses. The ultramafic rocks in the Zhimafang area are serpentinized phlogopite-bearing garnet lherzolite. Equilibrium conditions of the garnet lherzolite are estimated at about  $T = 750\text{--}850\text{ }^{\circ}\text{C}$  and  $P = 20\text{--}30\text{ kbar}$  (Zang et al., in prep.). The ultramafic rocks in the Mengzhong area are completely serpentinized. Bulk chemical analyses of the magnesian staurolite-bearing rocks are given in Table 1.

### Zhimafang samples

The Zhimafang samples (TS-03 and TS-04) are composed of a corundum-rich pink part and garnet-rich white part. The samples contain garnet and corundum with subordinate amounts of Na-rich phlogopite, zoisite, pentlandite, and apatite as primary minerals. Aggregates of fine-grained diaspore, margarite, dolomite, and calcite (all  $<0.03\text{ mm}$  in size) were observed as inclusions in corundum crystals. Secondary minerals are magnesian staurolite, Al-rich pargasite, chlorite, clinozoisite, Mg-rich albanite, and heazlewoodite ( $\text{Ni}_3\text{S}_2$ ).

Both garnet and corundum occur as anhedral crystals  $0.1\text{--}2.0\text{ mm}$  in size. They are usually surrounded by aggregates of magnesian staurolite and chlorite. Garnet is partly replaced by Al-rich pargasite and clinozoisite around the crystal rim and along fractures. Phlogopite shows a subhedral and tabular form and is partly replaced by chlorite. Magnesian staurolite constitutes acicular and/or prismatic crystals and forms pseudomorphs after garnet and corundum with chlorite (Fig. 2).

The bulk chemistry of the garnet-corundum rock (TS-03) is characterized by an extremely high  $\text{Al}_2\text{O}_3/\text{SiO}_2$  val-

TABLE 1. Bulk chemical compositions of magnesian staurolite-bearing rocks

	TS-03†		TM-02			
	Wt%	Wt%	Wt%	Norm		
$\text{SiO}_2$	34.26	47.0	Or	0.1		
$\text{TiO}_2$	0.02	0.58	Ab	6.9		
$\text{Al}_2\text{O}_3$	34.87	14.1	An	34.8		
$\text{Cr}_2\text{O}_3$	0.31	0.79	Di	25.6	En	9.5
$\text{Fe}_2\text{O}_3$	0.58				Fs	2.7
FeO	4.14	7.76*			Wo	13.4
MnO	0.18	0.12	Hy	13.5	En	10.5
MgO	13.40	14.3			Fs	3.0
NiO	n.d.	0.05	Ol	14.3	Fo	10.9
CaO	10.90	13.5			Fa	3.4
$\text{Na}_2\text{O}$	0.15	0.81	Mt	1.6		
$\text{K}_2\text{O}$	0.05	0.02	Cm	1.2		
$\text{P}_2\text{O}_5$	0.33	0.01	Ilm	1.1		
$\text{H}_2\text{O}(+)$	0.32		Ap	0.0		
$\text{H}_2\text{O}(-)$	0.12					
Total	99.63	99.0		99.1		

Note: Normative composition of TM-02 was calculated on the basis of  $\text{Fe}^{3+}/\text{Fe}^{2+}$  ratio of 0.15.

\* Total Fe as FeO.

† Analyzed by Shiguang Wang.

ue (1.0) and low  $\text{Fe}_2\text{O}_3 + \text{FeO}$  content (4.7 wt%) and is similar to that of some diaspore bauxites (e.g., Valetton, 1972). This rock is also enriched in MgO and CaO. These components may have been derived from dolomite or dolomitic limestones, which are usually associated with bauxites. The garnet-corundum rocks are considered to be metamorphosed mixtures of bauxites and Mg-rich carbonate rocks, on the basis of the occurrence of diaspore and carbonate inclusions in the corundum crystals and the bulk chemistry of the garnet-corundum rock.

### Mengzhong sample

The Mengzhong sample (TM-02) is massive and consists of a clinopyroxene-rich green part and garnet-rich brown part. The sample contains garnet, clinopyroxene, and subordinate amounts of corundum, kyanite, zoisite, dolomite, rutile, and apatite as primary minerals. Secondary minerals are magnesian staurolite, calcic amphibole, clinozoisite, and chlorite.

Garnet occurs usually as euhedral or subhedral crystals  $0.1\text{--}0.5\text{ mm}$  in diameter. Large garnet crystals  $1\text{--}2\text{ cm}$  in diameter are sometimes observed. The garnet crystals are usually replaced by calcic amphibole, chlorite, and clinozoisite around crystal rims and along fractures. Clinopyroxene occurs as rounded and subhedral crystals  $0.1\text{--}0.5\text{ mm}$  in size in the matrix and as fine inclusions smaller than  $0.05\text{ mm}$  in size in the garnet crystals. Corundum is smaller than  $0.03\text{ mm}$  in size and is rimmed by chlorite. Kyanite forms anhedral crystals smaller than  $0.02\text{ mm}$  in size and is replaced by magnesian staurolite and calcic amphibole. Zoisite shows prismatic forms  $0.1\text{--}0.3\text{ mm}$  in length and occurs usually as inclusions in garnet. Some zoisite crystals contain fine-grained garnet inclusions smaller than  $0.03\text{ mm}$  in size. Magnesian staurolite forms anhedral crystals smaller than  $0.02\text{ mm}$  in size and

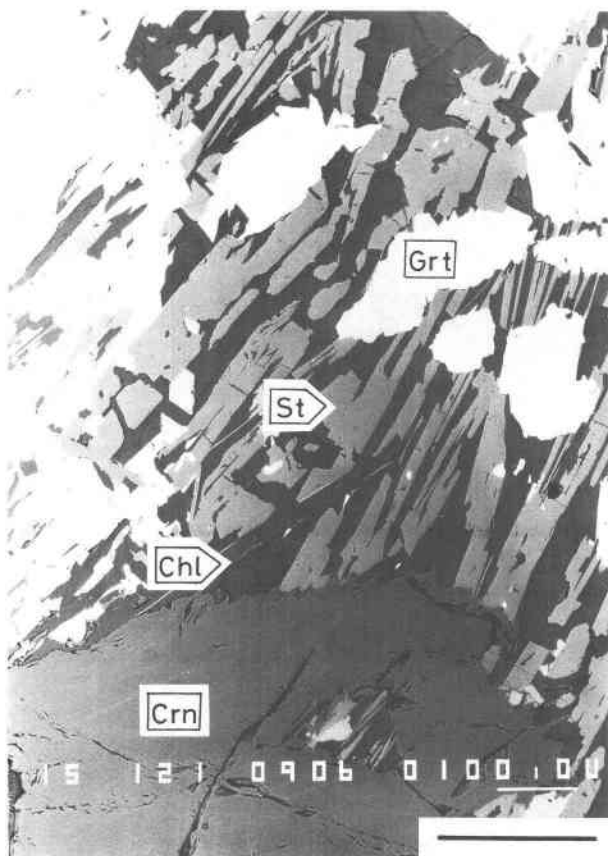


Fig. 2. Backscattered-electron image of magnesian staurolite and other constituents (sample TS-04). Scale bar indicates 200  $\mu\text{m}$ . Abbreviations for minerals: St, magnesian staurolite; Grt, garnet; Crn, corundum; Chl, chlorite.

occurs as pseudomorphs after kyanite. Magnesian staurolite crystals are partly surrounded by calcic amphibole.

The garnet + clinopyroxene + corundum assemblage of the Mengzhong eclogite suggests equilibrium conditions of  $T = 700\text{--}750\text{ }^\circ\text{C}$  and  $P = 11\text{--}25\text{ kbar}$  for the primary stage (Enami et al., 1986). Its bulk and mineral compositions are similar to those of eclogite xenoliths in kimberlites (Tables 1 and 3; also cf. Dawson, 1980). These data suggest that the Mengzhong eclogite was generated from the lower crust or upper mantle.

#### MINERALOGY OF MAGNESIAN STAUKROLITE AND ASSOCIATED MINERALS

Chemical analyses were performed with a JEOL electron-probe microanalyzer (EPMA) JXA-733. Accelerating voltage, specimen current, and beam diameter were kept at 15 kV,  $1.2 \times 10^{-8}\text{ A}$  and 3  $\mu\text{m}$ , respectively. Chemical compositions of the magnesian staurolite and other constituent minerals are given in Tables 2 and 3, respectively.

#### Magnesian staurolite

**Chemistry.**  $\text{H}_2\text{O}$  content of staurolite is variable and cannot be associated with a fixed stoichiometry (e.g., Juurinen, 1956; Lonker, 1983; Holdaway et al., 1986a). Li is sometimes concentrated in staurolite (Hietanen, 1969; Grew and Sandiford, 1984; Holdaway et al., 1986b; Dutrow et al., 1986).  $\text{H}_2\text{O}$  and  $\text{Li}_2\text{O}$  contents cannot be estimated by EPMA analysis, and so the chemical formula of the magnesian staurolite was calculated on the basis of  $\text{Si} + \text{Al} + \text{Cr} = 25.53$  as recommended by Holdaway et al. (1986b).  $\text{V}_2\text{O}_3$ ,  $\text{ZnO}$ ,  $\text{CoO}$ ,  $\text{CaO}$ ,  $\text{Na}_2\text{O}$ , and  $\text{K}_2\text{O}$  contents of the magnesian staurolite are below the detection limits, i.e., less than 0.02 wt% for  $\text{V}_2\text{O}_3$  and less than 0.01 wt% for the other elements.

The magnesian staurolite is faintly yellow in thin section and chemically homogeneous.  $X_{\text{Mg}}$  values [=  $\text{Mg}/(\text{Mg} + \text{Fe})$ ] of the magnesian staurolite are  $0.74 \pm 0.01$  and  $0.69 \pm 0.01$  in the Zhimafang and Mengzhong samples, respectively. Average Si content per formula unit is 7.92 for the Zhimafang samples and 7.74 for the Mengzhong sample. Grew and Sandiford (1984) pointed out that lower Si content is characteristic of Mg-rich staurolite from silica-undersaturated environments. Although the present samples contain corundum, the Si contents of these magnesian staurolites are higher than the Si contents of Mg-rich staurolite from other corundum-bearing samples (e.g., 7.43–7.68; Ward, 1984a). The magnesian staurolite here occurs as pseudomorphs after corundum and/or kyanite, and so the relatively high Si contents are probably due to disequilibrium with the associated aluminous minerals.  $\text{Cr}_2\text{O}_3$  contents of the magnesian staurolite are up to 0.70 and 1.17 wt% for the Zhimafang and Mengzhong samples, respectively.

Figure 3 explores the variation of cation contents in the staurolite monolayer, except for Al ( $FM$  content =  $\text{Fe} + \text{Mn} + \text{Mg} + \text{Zn} + \text{Co} + \text{Ni} + \text{Li} + \text{Ti}$ ), for staurolites reported in the literature. Figure 3 clearly shows that the  $FM$  content of staurolite increases with increase in  $Y_{\text{Mg}}$  value (=  $\text{Mg}/FM$ ). The  $FM$  content of Mg-rich staurolites ( $Y_{\text{Mg}} \geq 0.4$ ) is higher than 4.0, and its average is 4.6. The  $FM$  content of Mg-poor staurolites ( $Y_{\text{Mg}} \leq 0.2$ ) is mostly lower than 4.2, and its average is 3.9. Two Mg-poor staurolites with  $FM > 4.6$  were reported by Griffen and Ribbe (1973) (specimens 4 and 10), and the latter has a high ZnO content of 6.86 wt%. Staurolites with  $Y_{\text{Mg}} = 0.2\text{--}0.4$  have compositions intermediate between the above two groups (average  $FM$  content is 4.2), except for the unusually Zn-enriched staurolites with ZnO = 7.44 and 6.73 wt% reported by Juurinen (1956) and Miyake (1985), respectively. The compositional variation seen in Figure 3 may have some uncertainties because of the absence of  $\text{H}_2\text{O}$  and/or  $\text{Li}_2\text{O}$  data in most analyses. Thirty complete analyses of staurolite,<sup>1</sup> including  $\text{H}_2\text{O}$  and  $\text{Li}_2\text{O}$ , by Holdaway et al. (1986b), however, also show that the

<sup>1</sup> Excluding one analysis (specimen 6-3), believed to be inaccurate owing to variability in Li content (Dutrow et al., 1986).

TABLE 2. Chemical compositions of magnesian staurolites

	Zhimaifang			Mengzhong		
	TS-03		C-2†	TS-04	TM-02	
	n = 17‡	C-1†		n = 20‡	n = 7‡	Cr‡
SiO <sub>2</sub>	29.8(0.3)	29.8	29.5	29.9(0.4)	28.5(0.2)	28.1
TiO <sub>2</sub>	0.00	0.00	0.00	0.00	0.25(0.06)	0.33
Al <sub>2</sub> O <sub>3</sub>	55.9(0.4)	55.8	56.2	56.1(0.4)	55.0(0.5)	54.4
Cr <sub>2</sub> O <sub>3</sub>	0.53(0.08)	0.53	0.57	0.54(0.09)	0.83(0.21)	1.17
FeO*	4.69(0.21)	4.70	4.60	4.76(0.19)	5.92(0.10)	6.09
MnO	0.07(0.03)	0.09	0.10	0.03(0.03)	0.00	0.00
MgO	7.38(0.07)	7.37	7.35	7.50(0.15)	7.36(0.11)	7.33
NiO	0.16(0.05)	0.14	0.11	0.16(0.03)	0.00	0.00
CaO	0.00	0.00	0.00	0.00	0.00	0.00
Na <sub>2</sub> O	0.00	0.00	0.00	0.00	0.00	0.00
K <sub>2</sub> O	0.00	0.00	0.00	0.00	0.00	0.00
Total	98.5	98.4	98.4	99.0	97.9	97.4
Formulae (Si + Al + Cr = 25.53)						
Si	7.917	7.927	7.830	7.915	7.743	7.703
Al	17.502	17.492	17.580	17.502	17.609	17.574
Ti	0.000	0.000	0.000	0.000	0.051	0.068
Cr	0.111	0.111	0.120	0.113	0.178	0.254
Fe <sup>2+</sup> *	1.042	1.045	1.021	1.054	1.345	1.396
Mn	0.016	0.020	0.022	0.007	0.000	0.000
Mg	2.922	2.923	2.908	2.960	2.981	2.995
Ni	0.034	0.030	0.023	0.034	0.000	0.000
Ca	0.000	0.000	0.000	0.000	0.000	0.000
Na	0.000	0.000	0.000	0.000	0.000	0.000
K	0.000	0.000	0.000	0.000	0.000	0.000
X <sub>Mg</sub> ‡	0.74	0.74	0.74	0.74	0.69	0.68

Note: Values in parentheses are the standard deviations.

\* Total Fe as FeO.

† n, number of analytical points; C-1 and C-2, crystals 1 and 2 for the X-ray analysis, respectively;

Cr, most Cr-rich composition.

‡ X<sub>Mg</sub> = Mg/(Mg + Fe).

*FM* content increases with increasing  $Y_{Mg}$  value in staurolite: average *FM* content of nine staurolites with  $Y_{Mg} \geq 0.2$  is 4.5 and that of three staurolites with  $Y_{Mg} \leq 0.1$  is 3.8. High *FM* content of some staurolites can be possibly explained by substitution of  ${}^VIAl$  by  $Fe^{3+}$ , which would be seen as part of the *FM* components (Holdaway et al., 1986b). Most of Mg-rich staurolites with  $Y_{Mg} \geq 0.4$ , however, coexist with zoisite or  $Fe^{3+}$ -poor clinozoisite ( $Fe_2O_3 = 2.33\text{--}4.2$  wt%) and probably have little  $Fe^{3+}$ . Staurolite of high  $Y_{Mg}$  tends to be lower in  ${}^VIAl$  content and vice versa: Average  ${}^VIAl$  contents are 17.3 and 17.6 for staurolites with  $Y_{Mg} \geq 0.2$  and  $Y_{Mg} \leq 0.1$ , respectively (Holdaway et al., 1986b). Thus the high *FM* content of Mg-rich staurolite suggests the preferential Mg substitution for  ${}^VIAl$ . Alternative explanations for the  ${}^VIAl = Mg$  substitution are  $2{}^VIAl = 3 Mg$  (see Ward, 1984a) or  ${}^VIAl = Mg + H$ .

Lonker (1983) showed the negative correlation between  ${}^VIAl$  and  $(Fe + Mg) + OH$  contents. This negative correlation implies that the second substitution scheme better explains Mg enrichment in staurolite. The present magnesian staurolite has lower *FM* (4.0–4.4) and lower Fe (1.1–1.3) concentrations than those of other Mg-rich staurolites. This fact suggests that the  $Fe = Mg$  substitution in the  ${}^{IV}Fe$  sites also affects the high Mg content of the magnesian staurolite concerned. The Mg substitution

in the  ${}^{IV}Fe$  sites is attributed to the extremely high  $X_{Mg}$  values of host rocks (0.84 for TS-03 and 0.77 for TM-02).

**X-ray data.** The magnesian staurolite was examined on a Rigaku RAD- $\gamma B$  X-ray microdiffractometer with position-sensitive proportional counter (PSPC/MDG system), using V-filtered  $CrK\alpha$  radiation ( $\lambda = 2.29092 \text{ \AA}$ , 40 kV, 200 mA). X-ray diffraction data were obtained from the two selected areas of about  $30 \mu m$  in diameter for two crystals in a thin section. Average chemical compositions of the selected areas obtained by EPMA analyses are shown in Table 2.

The X-ray diffraction data are summarized in Table 4. Peaks were indexed with respect to Schreyer and Seifert (1969) and Borg and Smith (1969). Diffractions with  $d > 6.6 \text{ \AA}$  could not be observed, since  $2\theta$  of the microdiffractometer ranged from  $20^\circ$  to  $140^\circ$  in the present study. Preliminary X-ray powder-diffraction analysis of a mixture of the magnesian staurolite and garnet crystals showed a weak peak at  $d = 8.34 \text{ \AA}$ , corresponding to the 020 reflection of the magnesian staurolite. Observed peaks and their intensities are different between the two selected areas, because of the limited oscillation angles around  $\phi$  and  $\chi$  axes of the microdiffractometer. Peak positions of the present study correspond well to those of Fe-free staurolite synthesized by Schreyer and Seifert (1969). An or-

TABLE 3. Chemical compositions of other constituent minerals

	TS-03				TS-04				TM-02				
	Phl n = 5	Mar	Grt n = 14	Crn Cr	Cam Al	Chl n = 9	Ala Mg	Grt n = 60	Grt Cr	Cpx n = 18	Ky Cr	Crn Cr	Zo Cr
SiO <sub>2</sub>	39.7	30.3	42.5	0.00	42.3	28.9	32.9	41.5	41.1	55.9	37.0	0.05	39.5
TiO <sub>2</sub>	0.00	0.00	0.00	0.00	0.00	0.00	0.02	0.05	0.11	0.00	0.00	0.06	0.06
Al <sub>2</sub> O <sub>3</sub>	19.6	50.5	23.6	99.7	22.4	22.8	19.0	22.6	21.0	3.04	61.9	98.3	31.3
Cr <sub>2</sub> O <sub>3</sub>	0.26	0.46	0.34	1.10	0.31	0.32	n.d.	0.63	2.92	0.54	1.18	0.89	1.59
FeO*	1.76	0.08	5.07	0.25**	3.31	2.38	1.39	12.6	12.4	1.75	0.50**	0.35**	1.53**
MnO	0.00	0.00	0.14	0.00	0.05	0.00	0.06	0.23	0.23	0.00	0.06	0.00	0.06
MgO	24.0	0.06	15.8	0.02	15.1	31.8	6.20	14.0	13.4	15.1	0.24	0.00	0.13
NiO	0.81	0.09	0.00	0.00	0.06	0.75	n.d.	0.03	0.00	0.14	0.00	0.00	0.07
CaO	0.00	13.7	13.4	0.00	13.1	0.00	11.0	8.84	10.2	21.9	0.00	0.00	23.9
Na <sub>2</sub> O	2.66	0.18	0.00	0.00	2.44	0.03	0.00	0.00	0.00	2.02	0.00	0.00	0.00
K <sub>2</sub> O	7.21	0.00	0.00	0.00	0.00	0.00	0.00	0.00	0.00	0.00	0.00	0.00	0.00
Total	96.0	95.4	100.9	101.1	99.1	87.0	98.6§	100.5	101.4	100.4	100.9	99.7	98.1
	O = 22	O = 22	O = 12	O = 3	O = 23	O = 28	Formulae	O = 12	O = 12	O = 6	O = 5	O = 3	O = 12.5
Si	5.478	4.028	3.011	0.000	5.849	5.450	2.996	3.021	3.000	2.005	0.996	0.001	3.012
Al	3.187	7.911	1.970	1.982	3.650	5.067	2.033	1.939	1.806	0.128	1.967	1.981	2.813
Ti	0.000	0.000	0.000	0.000	0.000	0.000	0.001	0.003	0.006	0.000	0.000	0.001	0.003
Cr	0.028	0.048	0.019	0.015	0.034	0.048	n.d.	0.036	0.168	0.015	0.025	0.012	0.096
Fe <sup>2+</sup> **	0.203	0.009	0.300	0.003**	0.383	0.375	0.088	0.767	0.757	0.052	0.010**	0.005**	0.088**
Mn	0.000	0.000	0.008	0.000	0.006	0.000	0.000	0.014	0.014	0.000	0.001	0.000	0.004
Mg	4.936	0.012	1.668	0.001	3.112	8.938	0.839	1.519	1.458	0.807	0.010	0.000	0.015
Ni	0.090	0.010	0.000	0.000	0.007	0.114	n.d.	0.002	0.000	0.004	0.000	0.000	0.004
Ca	0.000	1.951	1.017	0.000	1.941	0.000	1.070	0.689	0.798	0.841	0.000	0.000	1.952
Na	0.712	0.046	0.000	0.000	0.654	0.000	n.d.	0.000	0.000	0.140	0.000	0.000	0.000
K	1.269	0.000	0.000	0.000	0.000	0.000	0.000	0.000	0.000	0.000	0.000	0.000	0.000
X <sub>Mg</sub> †	0.96		0.85		0.89	0.96		0.66	0.66	0.94			
REE‡							0.945						
X <sub>Ca</sub>													0.30

Note: Abbreviations are Phl, phlogopite; Mar, margarite; Grt, garnet; Crn, corundum; Cam, calcic amphibole; Chl, chlorite; Ala, allanite; Cpx, clinopyroxene; Ky, kyanite; Zo, zoisite; n, number of analytical points; Cr, most Cr-rich composition; Al, most Al-rich composition; Mg, most Mg-rich composition; n.d., not determined.

\* Total Fe as FeO.

\*\* Total Fe as Fe<sub>2</sub>O<sub>3</sub>.

† X<sub>Mg</sub> = Mg/(Mg + Fe).

‡ Includes La<sub>2</sub>O<sub>3</sub>, 9.49; Ce<sub>2</sub>O<sub>3</sub>, 12.3; Pr<sub>2</sub>O<sub>3</sub>, 2.83; Nd<sub>2</sub>O<sub>3</sub>, 1.95; Sm<sub>2</sub>O<sub>3</sub>, 0.11; and Ge<sub>2</sub>O<sub>3</sub>, 1.36 wt%.

|| X<sub>Ca</sub> = Fe<sup>3+</sup>/(Fe<sup>3+</sup> + Al).

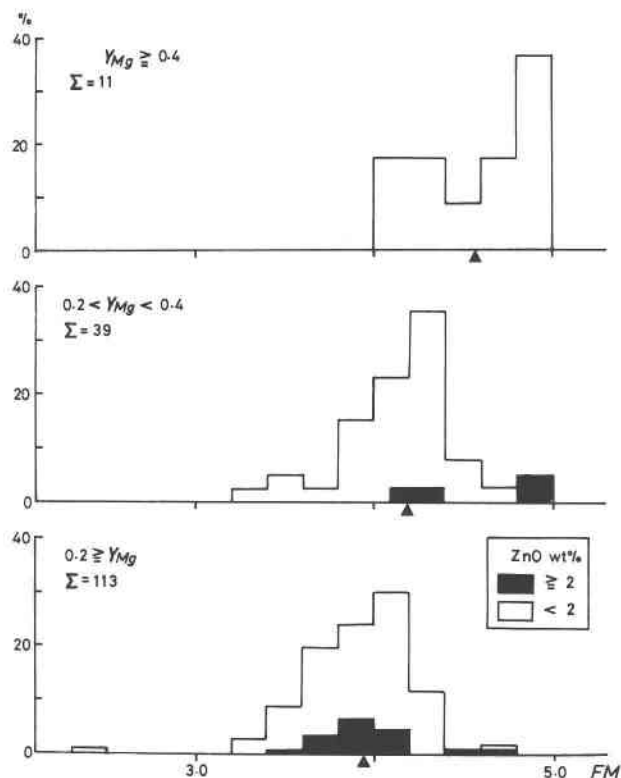


Fig. 3. Variations of  $FM$  ( $= Fe + Mn + Mg + Zn + Co + Ni + Li + Ti$ ) content of staurolites. Solid triangles indicate average  $FM$  contents. Data are from Asami and Hoshino (1980), Asami et al. (1982), Ashworth (1975), Baltatzis (1979), Cěch et al. (1981), Enami and Zang (this paper), Foster (1977), Fox (1971), Gibson (1978), Green (1963), Grew and Sandiford (1984), Griffen and Ribbe (1973), Guidotti (1970), Hietanen (1969), Hiroi (1983), Hollister (1970), Hollister and Bence (1967), Hounslow and Moore (1967), Hudson (1980), Juurinen (1956), Kwak (1974), Lonker (1983), Miyake (1985), Pigage (1976), Schreyer and Chinner (1966), Schreyer et al. (1984), Smith (1968), Takéuchi et al. (1972), von Knorring et al. (1979), and Ward (1984a, 1984b).

TABLE 4. X-ray data of magnesian staurolite in TS-03

Crystal 1		Crystal 2		$d_{calc}$	$h$	$k$	$l$
$d_{obs}$	$l/l_0$	$d_{obs}$	$l/l_0$				
4.53	10			4.52	1	3	0
4.43	<5	4.45	20	4.42	1	1	1
3.549	40			3.555	2	2	0
		3.527	25	3.526	1	3	1
		3.225	40	3.227	2	0	1
3.048	15			3.052	1	5	0
3.002	55	3.007	95	3.007	2	2	1
2.846	15			2.853	2	4	0
2.683	65			2.684	1	5	1
		2.618	5	2.620	1	1	2
2.542	55	2.542	20	2.545	2	4	1
		2.387	100	2.392	1	3	2
2.366	100			2.370	3	3	0
		2.351	60	2.355	3	1	1
		2.289	30	2.292	2	0	2
2.257	30			2.260	2	6	0
2.099	30	2.097	5	2.102	1	7	1
2.069	<5	2.069	5	2.070	0	8	0
2.054	10			2.057	3	5	0
2.003	<5			2.005	-2	4	2
		1.857	10	1.858	4	0	1
1.776	5			1.778	4	4	0
1.765	<5	1.763	<5	1.766	1	7	2
1.706	10			1.707	1	9	1
		1.660	10	1.661	2	2	3
		1.600	15	1.600	1	5	3
1.570	5			1.569	2	4	3
1.542	10	1.542	35	1.541	4	6	1
		1.538	30	1.536	2	8	2
1.514	70			1.514	5	3	0
		1.511	75	1.512	1	9	2
1.474	15	1.473	5	1.473	2	10	1
1.447	15	1.446	30	1.446	1	7	3
1.429	10			1.428	0	10	2
		1.423	5	1.422	5	5	0
1.378	5			1.380	0	12	0
1.371	5			1.370	5	1	2
1.312	<5						
		1.310	5				
		1.296	5				
1.279	<5						
1.273	<5						
		1.267	10				
1.264	10						
1.255	5						
1.239	<5	1.239	10				
		1.221	10				

thorhombic cell was assumed, and unit-cell dimensions calculated on the basis of 30 reflection data with  $44^\circ < 2\theta < 120^\circ$  (excluding  $0k0$  reflections) are as follows:  $a = 7.873(3)$  Å,  $b = 16.557(7)$  Å, and  $c = 5.637(3)$  Å. The  $a$  and  $c$  axes are similar to those of staurolites in the literature ( $a = 7.850$ – $7.891$  Å and  $c = 5.635$ – $5.667$  Å). Griffen et al. (1982) showed that the  $b$  axis of staurolite decreases systematically with decreasing mean ionic radius (MIR) of cations in the monolayer. The  $b$  axis of the magnesian staurolite (TS-03) lies close to the regression line of that against the MIR value (Fig. 4).

#### Garnet, clinopyroxene, and calcic amphibole

The garnet is mostly homogeneous and belongs to a grossular-rich pyrope-almandine series with very low MnO content (less than 0.3 wt%). Average compositions in terms

of garnet end members are  $Prp_{54.5}Alm_{10.0}Grs_{35.3}Sps_{0.2}$ ,  $Prp_{55.7}Alm_{10.0}Grs_{34.0}Sps_{0.3}$ , and  $Prp_{50.8}Alm_{25.7}Grs_{23.1}Sps_{0.5}$  for TS-03, TS-04, and TM-02, respectively (abbreviations after Kretz, 1983). The  $Cr_2O_3$  content of TM-02 garnet reaches 2.9 wt% in the crystal core. The clinopyroxene is pale green in hand specimen, considering its substantial  $Cr_2O_3$  content (0.63 wt% maximum), and is sodian augite ( $Na_2O = 2.0 \pm 0.3$  wt%,  $X_{Mg} = 0.94$ ) of Essene and Fyfe (1967). The amphibole varies in composition from flake to flake. In the TM-02, the amphibole replacing garnet is magnesiohornblende with  $Al_2O_3 = 12.0 \pm 2.1$  wt% and that replacing the magnesian staurolite is tschermakite with maximum  $Al_2O_3$  of 18.8 wt%, according to the nomenclature of Leake (1978). The amphibole in the Zhi-mafang samples is Al-rich pargasite, and its  $Al_2O_3$  content is up to 22.4 wt%.

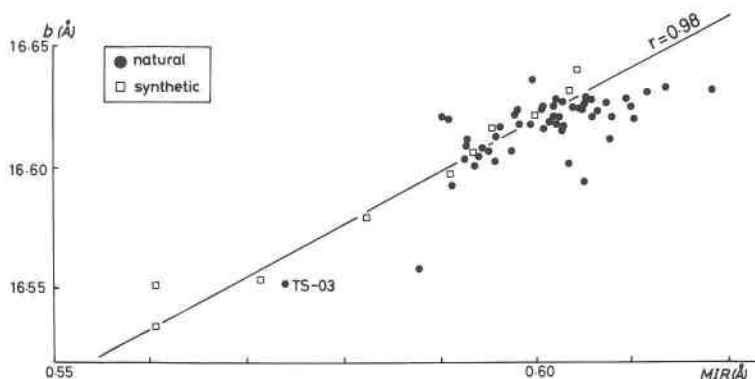


Fig. 4. Relationship between mean ionic radius (MIR) of cations in the monolayer and  $b$  axis of staurolite. Regression line plotted was calculated using ten data of synthetic staurolites. Ionic radii were taken from Griffen (1981) for Zn and from Shannon (1976) for the other elements;  $r$  = correlation coefficient. Data are from Čech et al. (1981), Enami and Zang (this study), Griffen and Ribbe (1973), Juurinen (1956), Miyake (1985), Schreyer and Chinner (1966), Smith (1968), Takéuchi et al. (1972), von Knorring et al. (1979), and Ward (1984a) for natural staurolites and from Griffen (1981), Richardson (1966), and Schreyer and Seifert (1969) for synthetic staurolites.

### Corundum and kyanite

Corundum is a pink variety owing to its high  $\text{Cr}_2\text{O}_3$  content, up to 1.1 wt% in the Zhimafang samples and 0.9 wt% in the Mengzhong sample. Its  $\text{Fe}_2\text{O}_3$  content is less than 0.4 wt%. Kyanite is also enriched in  $\text{Cr}_2\text{O}_3$  (1.2 wt% maximum), and its  $\text{Fe}_2\text{O}_3$  content is  $0.4 \pm 0.1$  wt%.

### Phlogopite, chlorite, and margarite

Both phlogopite and chlorite have high  $X_{\text{Mg}}$  values of about 0.96 and are colorless in thin section. Phlogopite is unusually enriched in  $\text{Na}_2\text{O}$  ( $2.7 \pm 0.2$  wt%). NiO contents of phlogopite and chlorite in the Zhimafang samples are up to 1.0 and 1.1 wt%, respectively. Margarite is depleted in both  $\text{Na}_2\text{O} + \text{K}_2\text{O}$  (0.18 wt%) and  $\text{FeO} + \text{MgO}$  (0.1 wt%).

### Epidote group minerals

Both zoisite and clinozoisite are colorless in thin section.  $X_{\text{Fe}^{3+}}$  values [ $= \text{Fe}^{3+}/(\text{Fe}^{3+} + \text{Al})$ ] of Zhimafang and Mengzhong zoisites are 0.030 and 0.035, respectively.  $\text{Cr}_2\text{O}_3$  content of the latter reaches 1.6 wt%. Clinozoisite is depleted in  $\text{Fe}^{3+}$ , and  $X_{\text{Fe}^{3+}}$  values are about 0.10 and 0.11 for the Zhimafang and Mengzhong samples, respectively. Allanite in the Zhimafang sample is pale brown and shows a weak compositional zoning consisting of REE-rich cores and Ca-rich rims. CaO and REE contents are 10.9 and 28.0 wt% in the crystal core and 12.5 and 24.5 wt% in the crystal rim, respectively. The MgO content of allanite reaches 6.2 wt%, and total Fe as FeO is less than 2.1 wt%, suggesting the substitution  $\text{Ca} + \text{Al} = \text{REE} + \text{Mg}$ .

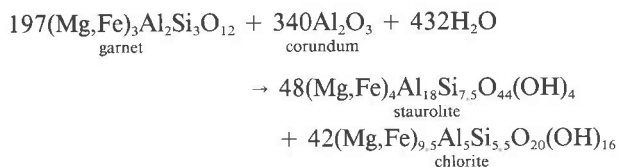
### Other minerals

Diaspore is enriched in  $\text{Cr}_2\text{O}_3$  (1.0 wt%), and its  $\text{Fe}_2\text{O}_3$  content is less than 0.6 wt%. Dolomite is homogeneous, and its average composition in terms of carbonate end members is  $\text{Ca}_{1.7}\text{Mg}_{0.43}\text{Sd}_0$  for the Zhimafang samples and

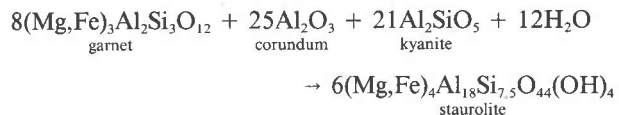
$\text{Ca}_{1.5}\text{Mg}_{0.47}\text{Sd}_2$  for the Mengzhong sample. Fe, Mn, and Mg components in calcite were not detected. Heazlewoodite is depleted in Fe (less than 0.1 wt%) and has a formula of  $\text{Ni}_{3.01}\text{S}_2$ .

### FORMATION OF MAGNESIAN STAULOLITES

Textural and chemical evidence shows that the magnesian staurolites in these rocks are all retrograde products. The Zhimafang staurolite occurs as a pseudomorph after garnet and corundum and forms an aggregate with chlorite. The Mengzhong staurolite occurs as a pseudomorph after kyanite. Suggested reactions for the magnesian staurolite formations are as follows:



for the Zhimafang samples and



for the Mengzhong sample. Grossular component in garnet was probably consumed for the formation of calcic amphibole and clinozoisite.

For the Zhimafang samples, the equilibrium temperature of the primary garnet + corundum stage was estimated at about 800–850 °C by the garnet-biotite geothermometer (methods of Indares and Martignole, 1985, and Hoinkes, 1986). The temperature calculated using the Ferry and Spear (1978) calibration for the Ca- and Mn-free system is 680 °C. The lower temperature estimates with the latter calibration may result from high grossular

component of garnet (35.3 mol%). The lower pressure limit of the primary stage is about 11–14 kbar on the basis of the garnet + corundum assemblage (cf. Droop and Bucher-Nurminen, 1984) and the stability field of pyrope garnet (Schreyer and Seifert, 1969). Its upper pressure limit is probably defined by the equilibrium pressure of the host garnet-lherzolite of about 20–30 kbar. For the Mengzhong sample, the equilibrium conditions of the primary stage were estimated at  $T = 700\text{--}750\text{ }^{\circ}\text{C}$  and  $P = 11\text{--}25$  kbar (Enami et al., 1986). The estimated conditions of the primary stage may define the upper  $T$  and  $P$  limits of magnesian staurolite formation. The lower  $T$  and  $P$  limits of magnesian staurolite formation are estimated at about  $730\text{--}770\text{ }^{\circ}\text{C}$  and 11 kbar from the stability range of the magnesian staurolite + chlorite assemblage (cf. Schreyer and Seifert, 1969; Grew and Sandiford, 1984). Equilibrium conditions of the magnesian staurolite of this study are similar to those of other Mg-rich staurolites in the literature.

In the present study, magnesian staurolite occurs in two characteristic rock types. The Zhimafang magnesian staurolite occurs in highly aluminous and silica-undersaturated rocks. The Mengzhong magnesian staurolite, on the other hand, occurs as a pseudomorph after kyanite in an eclogite without normative corundum. Schreyer (1967) suggested that the lack of natural magnesian staurolite was due to the absence of rocks having highly aluminous bulk compositions in the upper mantle where  $T$  and  $P$  conditions necessary for the formation of magnesian staurolite may prevail (i.e., higher than 11 kbar). He also pointed out that magnesian staurolite and quartz are incompatible by virtue of the stable tie lines between kyanite and other magnesian silicates. The Zhimafang samples, as well as most of Mg-rich staurolites in the literature, occur in metamorphosed peraluminous rocks such as sapphirine-garnet rock (Schreyer et al., 1984), corundum-bearing phlogopite-chlorite schist (Grew and Sandiford, 1984), and meta-anorthosite (Nicollet, 1986). These samples suggest that Mg-rich staurolite is formed in rocks having restricted bulk chemistry under limited  $T$  and  $P$  conditions. Mg-rich staurolite formation in typical mafic rocks may require much higher pressure reaching 24–26 kbar as shown by Hellman and Green (1979). The Mengzhong sample, however, clearly shows that Mg-rich staurolite can occur in common eclogite. Ward (1984a) reported Mg-rich staurolite in a reaction zone between plagioclase and orthopyroxene crystals in a metatroctolite. The Mengzhong sample and that of Wand thus suggest that Mg-rich staurolite can be formed in common metabasites by local reactions of aluminous and magnesian minerals.

The Mengzhong sample has bulk and mineral compositions similar to those of eclogite xenoliths in kimberlites (Enami et al., 1986). Kyanite and other aluminous minerals are common in high-pressure eclogites (e.g., Dawson, 1980), and local breakdown of these minerals with decreasing temperature may be expected to form Mg-rich staurolite. Hellman and Green (1979) suggested that stau-

rolite may be widespread in mafic rocks metamorphosed at high pressures, as, for example, in the subducted lithosphere. We also emphasize that careful petrographic examinations will probably reveal wide occurrence of Mg-rich staurolite as an accessory mineral in common metabasites formed under high pressures, especially in eclogites.

#### ACKNOWLEDGMENTS

We wish to express our sincere thanks to Professor K. Suwa of Nagoya University for his critical comments on the manuscript. Thanks are also due to Mr. S. Wang of Beijing University and Mr. M. Amemiya of Rigaku for their help in laboratory and to Mr. I. Hiraiwa of Nagoya University for preparing many thin sections. This study was supported in part by a Grant in Aid for Scientific Research from the Ministry of Education of Japan (No. 62740481: M.E.).

#### REFERENCES CITED

- Asami, M., and Hoshino, M. (1980) Staurolite-bearing schists from the Hongu-san area in the Ryoke metamorphic belt, central Japan. *Geological Society of Japan Journal*, 86, 581–591.
- Asami, M., Hoshino, M., Miyakawa, K., and Suwa, K. (1982) Metamorphic conditions of staurolite schists of the Ryoke metamorphic belt in the Hazu-Hongūsan area, central Japan. *Geological Society of Japan Journal*, 88, 437–450.
- Ashworth, J.R. (1975) Staurolite at anomalously high grade. *Contributions to Mineralogy and Petrology*, 53, 281–291.
- Baltatzis, E. (1979) Staurolite-forming reactions in the eastern Dalradian rocks of Scotland. *Contributions to Mineralogy and Petrology*, 69, 193–200.
- Borg, I.Y., and Smith, D.K. (1969) Calculated X-ray powder patterns for silicate minerals. *Geological Society of America Memoir* 122.
- Cěch, F., Povondra, P., and Vrana, S. (1981) Cobaltoan staurolite from Zambia. *Bulletin de Minéralogie*, 104, 526–529.
- Dawson, J.B. (1980) Kimberlites and their xenoliths. Springer-Verlag, New York.
- Deer, W.A., Howie, R.A., and Zussman, J. (1982) Rock-forming minerals, vol. 1A, Orthosilicates (2nd edition). Wiley, New York.
- Droop, G.T.R., and Bucher-Nurminen, K. (1984) Reaction textures and metamorphic evolution of sapphirine-bearing granulites from the Gruf complex, Italian central Alps. *Journal of Petrology*, 25, 766–803.
- Dutrow, B.L., Holdaway, M.J., and Hinton, R.W. (1986) Lithium in staurolite and its petrologic significance. *Contributions to Mineralogy and Petrology*, 94, 496–506.
- Enami, M., Wang, S., Zang, Q., and Hiraiwa, I. (1986) Eclogites from the Donghai district, Jiangsu province, east China. *Nagoya University Museum Bulletin*, no. 2, 55–70.
- Essene, E.J., and Fyfe, W.S. (1967) Omphacite in Californian metamorphic rocks. *Contributions to Mineralogy and Petrology*, 15, 1–23.
- Ferry, J.M., and Spear, F.S. (1978) Experimental calibration of the partitioning of Fe and Mg between biotite and garnet. *Contributions to Mineralogy and Petrology*, 66, 113–117.
- Foster, C.T., Jr. (1977) Mass transfer in sillimanite-bearing pelitic schists near Rangeley, Maine. *American Mineralogist*, 62, 727–746.
- Fox, J.S. (1971) Coexisting chloritoid and staurolite and the staurolite-chlorite isograd from the Agnew Lake area, Ontario, Canada. *Geological Magazine*, 108, 205–219.
- Gibson, G.M. (1978) Staurolite in amphibolite and hornblendite sheets from the Upper Seaforth river, central Fiordland, New Zealand. *Mineralogical Magazine*, 42, 153–154.
- Green, J.C. (1963) High-level metamorphism of pelitic rocks in northern New Hampshire. *American Mineralogist*, 48, 991–1023.
- Grew, E.S., and Sandiford, M. (1984) A staurolite-talc assemblage in tourmaline-phlogopite-chlorite schist from northern Victoria Land, Antarctica, and its petrogenetic significance. *Contributions to Mineralogy and Petrology*, 87, 337–350.
- Griffen, D.T. (1981) Synthetic Fe/Zn staurolites and the ionic radius of  $^{2+}\text{Zn}^{2+}$ . *American Mineralogist*, 66, 932–937.

- Griffen, D.T., and Ribbe, P.H. (1973) The crystal chemistry of staurolite. *American Journal of Science*, 273-A, 479–495.
- Griffen, D.T., Gosney, T.C., and Phillips, W.R. (1982) The chemical formula of natural staurolite. *American Mineralogist*, 67, 292–297.
- Guidotti, C.V. (1970) The mineralogy and petrology of the transition from the lower to upper sillimanite zone in the Oquossoc area, Maine. *Journal of Petrology*, 11, 277–336.
- Hellman, P.L., and Green, T.H. (1979) The high pressure experimental crystallization of staurolite in hydrous mafic compositions. *Contributions to Mineralogy and Petrology*, 68, 369–372.
- Hietanen, A. (1969) Distribution of Fe and Mg between garnet, staurolite, and biotite in aluminum-rich schist in various metamorphic zones north of the Idaho batholith. *American Journal of Science*, 267, 422–456.
- Hiroi, Y. (1983) Progressive metamorphism of the Unazuki pelitic schists in the Hida terrane, central Japan. *Contributions to Mineralogy and Petrology*, 82, 334–350.
- Hoinkes, G. (1986) Effect of grossular-content in garnet on the partitioning of Fe and Mg between garnet and biotite: An empirical investigation on staurolite-zone samples from the Austroalpine Schneeberg complex. *Contributions to Mineralogy and Petrology*, 92, 393–399.
- Holdaway, M.J., Dutrow, B.L., Borthwick, J., Shore, P., Harmon, R.S., and Hinton, R.W. (1986a) H content of staurolite as determined by H extraction line and ion microprobe. *American Mineralogist*, 71, 1135–1141.
- Holdaway, M.J., Dutrow, B.L., and Shore, P. (1986b) A model for the crystal chemistry of staurolite. *American Mineralogist*, 71, 1142–1159.
- Hollister, L.S. (1970) Origin, mechanism, and consequences of compositional sector-zoning in staurolite. *American Mineralogist*, 55, 742–766.
- Hollister, L.S., and Bence, A.E. (1967) Staurolite: Sectoral compositional variations. *Science*, 158, 1053–1056.
- Hounslow, A.W., and Moore, J.M., Jr. (1967) Chemical petrology of Grenville schists near Fernleigh, Ontario. *Journal of Petrology*, 8, 1–28.
- Hudson, N.F.C. (1980) Regional metamorphism of some Dalradian pelites in the Buchan area, N.E. Scotland. *Contributions to Mineralogy and Petrology*, 73, 39–51.
- Indares, A., and Martignole, J. (1985) Biotite-garnet geothermometry in the granulite facies: The influence of Ti and Al in biotite. *American Mineralogist*, 70, 272–278.
- Juurinen, A. (1956) Composition and properties of staurolite. *Annales Academiae Scientiarum Fennicae, Series A, III Geology*, 47, 1–53.
- Kretz, R. (1983) Symbols for rock-forming minerals. *American Mineralogist*, 68, 277–279.
- Kwak, T.A.P. (1974) Natural staurolite breakdown reactions at moderate to high pressures. *Contributions to Mineralogy and Petrology*, 44, 57–80.
- Leake, B.E. (1978) Nomenclature of amphiboles. *American Mineralogist*, 63, 1023–1052.
- Lonker, S.W. (1983) The hydroxyl content of staurolite. *Contributions to Mineralogy and Petrology*, 84, 36–42.
- Miyake, A. (1985) Zn-rich staurolite from the Uvete area, central Kenya. *Mineralogical Magazine*, 49, 573–578.
- Nicollet, C. (1986) Saphirine et staurolite riche en magnésium et chrome dans les amphibolites et anorthosites à corindon du Vohibory Sud, Madagascar. *Bulletin de Minéralogie*, 109, 599–612.
- Pigage, L.C. (1976) Metamorphism of the Settler schist, southwest of Yale, British Columbia. *Canadian Journal of Earth Sciences*, 13, 405–421.
- Research Institute of Geology, Chinese Academy of Geological Sciences. (1982) Tectonic map of Asia, 1:8 000 000, The Cartographic Publishing House, China.
- Richardson, S.W. (1966) Staurolite. *Carnegie Institution of Washington Year Book* 65, 248–252.
- Schreyer, W. (1967) A reconnaissance study of the system  $MgO-Al_2O_3-SiO_2-H_2O$  at pressures between 10 and 25 kb. *Carnegie Institution of Washington Year Book* 66, 380–392.
- Schreyer, W., and Chinner, G.A. (1966) Staurolite-quartzite bands in kyanite quartzite at Big Rock, Rio Arriba County, New Mexico. *Contributions to Mineralogy and Petrology*, 12, 223–244.
- Schreyer, W., and Seifert, F. (1969) High-pressure phases in the system  $MgO-Al_2O_3-SiO_2-H_2O$ . *American Journal of Science*, 267-A, 407–443.
- Schreyer, W., Horrocks, P.C., and Abraham, K. (1984) High-magnesium staurolite in a sapphirine-garnet rock from the Limpopo Belt, Southern Africa. *Contributions to Mineralogy and Petrology*, 86, 200–207.
- Shannon, R.D. (1976) Revised effective ionic radii and systematic studies of interatomic distances in halides and chalcogenides. *Acta Crystallographica*, A32, 751–767.
- Smith, J.V. (1968) The crystal structure of staurolite. *American Mineralogist*, 53, 1139–1155.
- Takéuchi, Y., Aikawa, N., and Yamamoto, T. (1972) The hydrogen locations and chemical composition of staurolite. *Zeitschrift für Kristallographie*, 136, 1–22.
- Tectonic map compiling group, Institute of Geology, Academia Sinica. (1974) A preliminary note on the basic tectonic features and their developments in China. *Scientia Geologica Sinica*, 1, 1–17.
- Valeton, I. (1972) Bauxites. In *Developments in soil science 1*, Elsevier, New York.
- von Knorring, O., Sahama, Th.G., and Siivola, J. (1979) Zincian staurolite from Uganda. *Mineralogical Magazine*, 43, 446.
- Ward, C.M. (1984a) Magnesium staurolite and green chromian staurolite from Fiordland, New Zealand. *American Mineralogist*, 69, 531–540.
- (1984b) Titanium and the color of staurolite. *American Mineralogist*, 69, 541–545.

MANUSCRIPT RECEIVED MAY 26, 1987

MANUSCRIPT ACCEPTED SEPTEMBER 2, 1987